Monthly Notices
of the
ROYAL ASTRONOMICAL SOCIETY

MNRAS **450,** 1916–1925 (2015) doi:10.1093/mnras/stv710

3C 57 as an atypical radio-loud quasar: implications for the radio-loud/radio-quiet dichotomy

J. W. Sulentic,[1]★ M. A. Martínez-Carballo,[1] P. Marziani,[2] A. del Olmo,[1] G. M. Stirpe,[3] S. Zamfir[4] and I. Plauchu-Frayn[1]†

[1]*Instituto de Astrofisíca de Andalucía, IAA-CSIC, Glorieta de la Astronomia s/n, Granada E-18008, Spain*
[2]*INAF–Osservatorio Astronomico di Padova, vicolo dell' Osservatorio 5, Padova I-35122, Italy*
[3]*INAF–Osservatorio Astronomico di Bologna, via Ranzani 1, Bologna I-40127, Italy*
[4]*Department of Physics & Astronomy, University of Wisconsin, WI 54481, Stevens Point, USA*

Accepted 2015 March 27. Received 2015 March 4; in original form 2014 December 15

ABSTRACT

Lobe-dominated radio-loud (LD RL) quasars occupy a restricted domain in the 4D Eigenvector 1 (4DE1) parameter space which implies restricted geometry/physics/kinematics for this subclass compared to the radio-quiet (RQ) majority of quasars. We discuss how this restricted domain for the LD RL parent population supports the notion for a RQ–RL dichotomy among type 1 sources. 3C 57 is an atypical RL quasar that shows both uncertain radio morphology and falls in a region of 4DE1 space where RL quasars are rare. We present new radio flux and optical spectroscopic measures designed to verify its atypical optical/UV spectroscopic behaviour and clarify its radio structure. The former data confirms that 3C 57 falls off the 4DE1 quasar 'main sequence' with both extreme optical Fe II emission ($R_{\rm Fe\,II} \sim 1$) and a large C IV λ1549 profile blueshift (~ -1500 km s^{-1}). These parameter values are typical of extreme Population A sources which are almost always RQ. New radio measures show no evidence for flux change over a 50+ year time-scale consistent with compact steep-spectrum (or young LD) over core-dominated morphology. In the 4DE1 context where LD RL are usually low $L/L_{\rm Edd}$ quasars, we suggest that 3C 57 is an evolved RL quasar (i.e. large blackhole mass) undergoing a major accretion event leading to a rejuvenation reflected by strong Fe II emission, perhaps indicating significant heavy metal enrichment, high bolometric luminosity for a low-redshift source and resultant unusually high Eddington ratio giving rise to the atypical C IV λ1549.

Key words: line: profiles – quasars: emission lines – quasars: general – quasars: individual: 3C 57.

1 INTRODUCTION

The origin of radio-loudness in quasars remains a perplexing question 50 years after their discovery. Ironically radio-loud (RL) quasars were the first to be discovered despite the fact that today they account for only 8 per cent of the low-redshift quasar population. After 50+ years, we do not know if RL quasars represent a distinct physical subset of the radio-quiet (RQ) quasar population or simply episodes through which all or most quasars pass. There is even confusion about the definition of an RL (or an RQ) quasar. In this paper, we simplify the problem by focusing only on low-redshift ($z \lesssim 0.7$) type 1 AGN/quasars that show broad (most in the range FWHM Hβ = 1000–12 000 km s^{-1}) emission line spectra including optical Fe II emission. We assume that they represent the parent population of highly accreting AGN and interpret them in the 4DE1 context (Sulentic, Marziani & Dultzin-Hacyan 2000a; Sulentic et al. 2007; Zamfir, Sulentic & Marziani 2008, hereafter Z08).

We can unambiguously define an RL type 1 quasar if we consider only the lobe-dominated (LD) RL sources which we assume to be the parent population of classical type 1 RL quasars. They show radio/optical flux ratios $R_{\rm K} > 70$, or better, $\log L_{1415\,\rm MHz} > 31.6$ erg s^{-1} Hz^{-1}. 'Better' because we avoid sensitivity of optical flux measures to internal extinction/galaxy orientation effects. No bona fide LD sources are found below our specified limits. Our RQ–RL boundary is set by the radio luminosities of the weakest sources showing LD radio morphology (Sulentic et al. 2003). At low redshift (z <0.7), LD structure is seen only in quasars with bolometric luminosity brighter than log $L_{\rm bol}$ = 44.0 erg s^{-1}. The 46 LD sources analysed by Z08 using an Sloan Digital Sky Survey (SDSS) DR5 subsample of 470 quasars ($z < 0.7$ and brighter than $g = 17.5$ or $i = 17.5$) show

★ E-mail: sulentic@iaa.es
† Currently at Instituto de Astronomía, UNAM, Ensenada, México.

© 2015 The Authors
Published by Oxford University Press on behalf of the Royal Astronomical Society

Downloaded from https://academic.oup.com/mnras/article-abstract/450/2/1916/983345 by guest on 12 March 2020

a radio luminosity range of nearly 3 dex ($\log L_{1415\mathrm{MHz}} = 31.7$–$34.4$ erg s^{-1} Hz^{-1}) and also a 3 dex optical range ($\log L_{\mathrm{bol}} = 44$–$47$ erg s^{-1}).

Core-dominated (CD) radio sources cannot be used to define an RQ–RL boundary because they span a radio luminosity range of 6 dex ($\log L_{1415\,\mathrm{MHz}} = 29$–$35$) from weak radio-detected RQ to the most luminous RL sources found in SDSS DR5 (Z08 supplemented by de Vries, Becker & White 2006). This corresponds to R_{K} values from less than 10 to several thousand. The highest luminosity CD sources are interpreted as relativistically boosted LD sources oriented preferentially to our line of sight. Such sources often show apparent superluminal motions (e.g. Zensus et al. 2002). As we proceed from the strongest towards weaker CD sources, and approach radio luminosities $\log L_{1415\,\mathrm{MHz}} \sim 31.6$ erg s^{-1} Hz^{-1}, the problem becomes acute. They are not luminous enough to be aligned or misaligned LD sources. Across our adopted RQ–RL boundary ($R_{\mathrm{K}} = 70$), only CD (and weak core-jet) sources are found and in numbers increasing with decreasing radio power. A survey of radio emission for PG quasars (Kellermann et al. 1989) led to a suggested RQ–RL boundary near $R_{\mathrm{K}} = 10$ using both LD and CD detections. The choice of this boundary rather than $R_{\mathrm{K}} = 70$ can have strong effects on statistical inferences when searching for differences between RL and RQ sources.

Contextualization can be helpful in relating quasar subclasses as well as the relation of individual sources to specific subclasses. Towards this goal, we adopted a 4D Eigenvector 1 (4DE1) parameter space (Sulentic et al. 2000a,b, 2007) based on four diagnostic measures: (1) full width half-maximum (FWHM) of broad (BC) Hβ; (2) flux ratio of optical FeII λ4570 blue blend and broad Hβ ($R_{\mathrm{Fe\,II}}$); (3) profile shift at half-maximum of high ionization C IV λ1549 c(1/2) and (4) soft X-ray photon index (Γ_{soft}). In the 4DE1 domain, RL sources do not distribute like the RQ majority but instead show a preference for FWHM H$\beta > 4000$ km s^{-1}, $R_{\mathrm{Fe\,II}} < 0.5$, unshifted C IV λ1549 profile and absence of a soft X-ray excess (i.e. $\Gamma_{\mathrm{soft}} \approx 2$). This is especially true for the LD RL parent population. Fig. 1 shows the 4DE1 optical plane for the SDSS DR5 quasar sample (Z08) with LD RL marked as filled red squares, luminous CD sources ($\log L_{1415\,\mathrm{MHz}} > 32.0$) as filled blue squares and RQ quasars as filled grey circles. We designate sources above and below FWHM H$\beta_{\mathrm{BC}} = 4000$ km s^{-1} as Population B (Pop B) and Population A (Pop A), respectively. The difference in 4DE1 domain occupation can be argued to be evidence that RL sources (the majority are Pop B) are fundamentally different from RQ quasars. However, this interpretation is complicated by the fact that ~40 per cent of RQ sources also occupy the same (Pop B) domain as the RL sources.

This paper considers an apparently non-conformist quasar 3C 57 ($z = 0.67$) that is unambiguously RL ($\log L_{1415\,\mathrm{MHz}} \approx 34.4$ erg s^{-1} Hz^{-1} and $\log R_{\mathrm{K}} \sim 3.0$). As such we expect it to show RL typical (average) 4DE1 parameter measures: (1) FWHM H$\beta_{\mathrm{BC}} \approx 6940$ km s^{-1}; (2) $R_{\mathrm{Fe\,II}} \approx 0.22$; (3) C IV λ1549 $c(\frac{1}{2}) \approx +50$ km s^{-1} and (4) $\Gamma_{\mathrm{soft}} \approx 2.15$ (Sulentic et al. 2007). In two of the four measures, 3C 57 is wildly discordant showing: $R_{\mathrm{Fe\,II}} \approx 1$ and C IV λ1549 blueshift $c(\frac{1}{2}) \approx -1500$ km s^{-1} (Sulentic et al. 2007, and this paper). These values are even extreme for RQ Pop A quasars. RQ sources have average values of C IV λ1549 $c(\frac{1}{2}) = -580$ km s^{-1} and $R_{\mathrm{Fe\,II}} \approx 0.48$ (Marziani et al. 1996; Sulentic et al. 2007; Richards et al. 2011).

New spectra were obtained for 3C 57 with three motivations: (1) to verify FWHM Hβ and confirm the previous unusually high $R_{\mathrm{Fe\,II}}$ measures, (2) to search for changes in the Hβ profile that are sometimes observed in RL sources (Corbin & Smith 2000) and

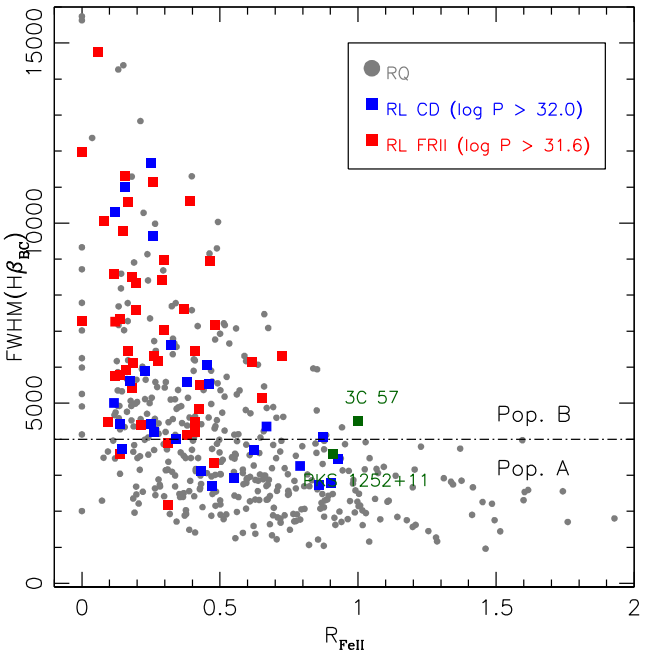


Figure 1. Location of 3C 57 in the optical plane of the 4DE1 space defined by FWHM Hβ_{BC} versus $R_{\mathrm{Fe\,II}}$. Filled red squares are LD RL sources, filled blue square CD RL sources following the definition of Z08 with weaker CD RL ($\log L_{1415\,\mathrm{MHz}} < 32.0$ erg s^{-1} Hz^{-1}) omitted for clarity. Filled grey circles correspond to RQ quasars.

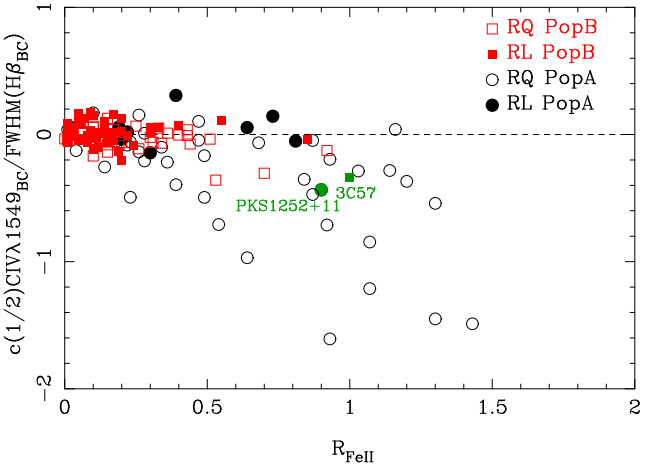


Figure 2. Location of 3C 57 and PKS 1252+11 in a 4DE1 UV-optical plane defined by normalized FWHM C IV λ1549 versus $R_{\mathrm{Fe\,II}}$. RL and RQ sources are marked as filled and open symbols, respectively. Pop A sources are represented by black circles while Pop B by red squares.

(3) to obtain high S/N line profile measures of Mg II λ2800 for use as a potentially more reliable black hole (BH) mass estimator (Marziani et al. 2013a,b). New radio observations were also obtained to shed light on the ambiguous morphological interpretations of 3C 57. It is very radio luminous and its apparent core-jet (CJ) structure leads us to expect flux variations over the 50+ year time span since its discovery.

The *Hubble Space Telescope (HST)* archive contained usable spectra for 130 low-z quasars as of late 2006 with a strong bias for RL sources. Fig. 2 shows a UV-optical plane of 4DE1 where FWHM normalized C IV λ1549 centroid shift is plotted against $R_{\mathrm{Fe\,II}}$. Open/filled black circles show RQ and RL Pop A quasars,

Downloaded from https://academic.oup.com/mnras/article-abstract/450/2/1916/983345 by guest on 12 March 2020

Table 1. 3C 57 optical observations.

Obs:	ORM	CAHA	Asiago
Tel	NOT 2.5 m	3.5 m	1.82 m
Instr.	ALFOSC	TWIN	AFOSC
Scale	0.19 arcsecpixel^{-1}	0.56 arcsec pixel^{-1}	0.26 arcsec pixel^{-1}
Grism	GR5	T13 and T11	GR4
Slit	1.3 arcsec	1.2 arcsec	1.26 arcsec
Disp	3.15 Å pixel^{-1}	2.14 Å pixel^{-1} 2.41 Å pixel^{-1}	4.92 Å pixel^{-1}
Range	5550–9400 Å	3400–5800 Å 5450–101 50 Å	3200–8200 Å
Date	29 Aug 2011	22 Oct 2012	05 Dec 2012
Texp	4 ×900 s	3 × 900 s	3 × 1200 s

respectively. RQ and RL Pop B sources are indicated by open/filled red squares. Six of the 59 RL sources in the *HST*-Faint Object Spectrograph (FOS) archival sample show a C IV λ1549 blueshift $c(\frac{1}{2})$ larger than 1000 km s^{-1}while the mean centroid shift value for the RL sources is +52km s^{-1}(Sulentic et al. 2007). If one normalizes the shift value by FWHM H$\beta_{\rm BC}$, we find two sources that stand out: 3C 57 and PKS 1252+11. This plot best illustrates the nature of 3C 57. We present here new radio and optical spectroscopic data that we hope will shed some light on the nature of 3C 57 (and PKS 1252+11) and why it (they) contravenes the clear trends in 4DE1. UV data have been taken from the *HST*-FOS archive and reanalysed. We use this to reconsider the definitions of radio-loudness.

New optical and radio observations are presented in Section 2 along with details of spectral analysis in 2.1. Section 3 presents results from analysis of new and literature data. Section 4 discusses the relation between RL quasars, C IV λ1549 blueshifts and the possible RQ–RL dichotomy. Section 4.3 considers how winds might be affected by radio outbursts while section 5 summarizes our inferences and conclusions.

2 OBSERVATIONS

New long slit optical spectroscopic observations of 3C 57 were carried out in three different telescopes: Calar Alto Observatory (CAHA, Almería Spain), El Roque de los Muchachos Observatory (ORM La Palma, Spain) and Asiago Observatory (Italy), in three different runs within a 15-month period. Table 1 summarizes the new data where we tabulate the instrumental setup for each observation as follows: telescope, spectrograph, spatial scale in arcsec/px, used grism, slit width in arcsec, spectral dispersion in Å pixel^{-1} and wavelength range. We also report the date of observation and the total integration time. The slit was oriented at parallactic angle to minimize effects of atmospheric differential refraction in the spectra. In the case of the TWIN spectrograph at CAHA with two arms, the observations were obtained simultaneously in the blue (grism #T13) and red (#T11) spectral regions. The three new spectra are plotted in Fig. 3 with CAHA, NOT and Asiago spectra shown in black, green and red, respectively. NOT and Asiago spectra have been vertically shifted to avoid confusion.

Data reduction was carried out in a standard way using the IRAF package. Spectra have been overscan corrected, nightly bias subtracted and flat-fielded with the normalized flat-field obtained after median combination of the flats. Wavelength calibration was obtained using standard lamp exposures. The APALL task was used for object extraction and background subtraction. Instrumental response and flux calibration were obtained each night through

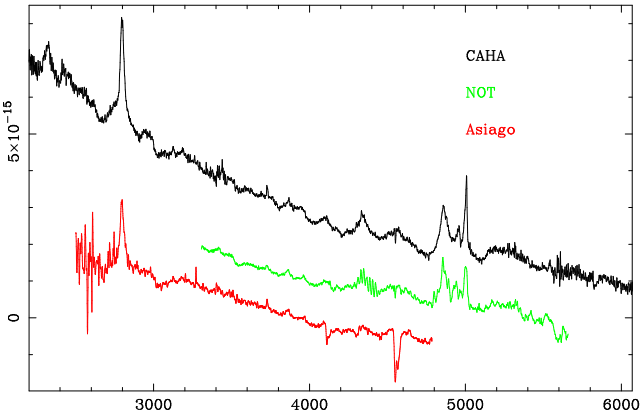


Figure 3. New spectra for 3C 57 covering Mg II λ2800 and Hβ in the rest frame. Abscissa is wavelength in Å and ordinate corresponds to specific flux in units of erg s^{-1} cm^{-2} Å^{-1}. NOT and Asiago spectra have been vertically displaced by -1×10^{-15} and -2×10^{-15} erg s^{-1} cm^{-2}, respectively for presentation.

Table 2. Radio measurements at 5 GHz.

Flux (mJy)	Reference
	3C 57
1390 ±80	Kuehr et al. 1981
1350	Wright et al. 1990
1372 ±72	Griffith et al. 1994
1441 ±30	This paper (observed in 2011)
	PKS 1252+11
1140 ±50	Kuehr et al. 1981
1030 ±70	Kuehr et al. 1981
641	VLA, Laurent-Muehleisen et al. 1997
961 ±30	This paper (observed in 2011)

observations of spectrophotometric standard stars from the list of Oke (1990) that we also use to remove telluric absorption bands.

New 5 GHz radio observations of 3C 57 were also carried out during 2011 November 14, using the single dish 32 m IRA-INAF antenna at Medicina in on-the-fly cross-scan mode. PKS 1252+11, the other known RL with a large C IV λ1549 blueshift, was also observed on 2011 November 15. Flux calibration was achieved using standard sources from the list of Ott et al. (1994). Fluxes and uncertainties that include calibrator uncertainty are reported in Table 2.

UV data have been taken from the *HST*-FOS archive. A reanalysis of UV spectra is presented in this paper. The 3C57 spectrum covers Si IV λ1397, C IV λ1549 and C III] λ1909 and was presented in Sulentic et al. (2007).

2.1 Multicomponent χ^2 analysis

All strong emission lines in the spectra were fitted using the IRAF task SPECFIT which employs a χ^2 minimization technique appropriate for non-linear multicomponent analysis (Kriss 1994). Marziani et al. (2009) provide a thorough description of analysis procedures for the optical spectral range; Marziani et al. (2013a,b) of the Mg II λ2800 range and Negrete et al. (2014) for the UV spectral range.

All broad components (BCs) were fitted with Lorentzian profiles and the remaining lines with Gaussians (see Section 3.2 for a justification of this procedure). The SPECFIT task adopted a power-law continuum dominating over any host galaxy contribution

Downloaded from https://academic.oup.com/mnras/article-abstract/450/2/1916/983345 by guest on 12 March 2020

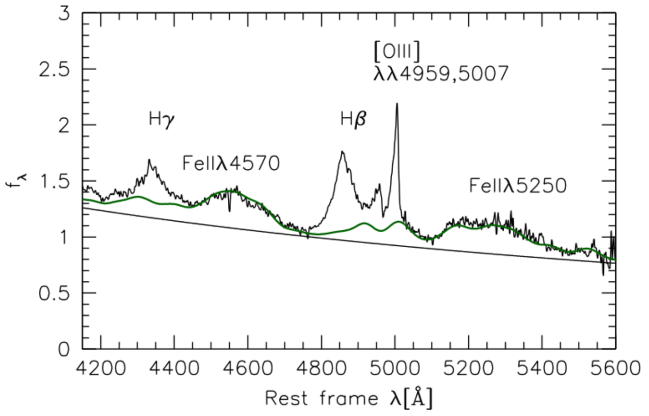


Figure 4. Continuum placement (filled line) for the normalized CAHA spectrum for the region of Hβ. Abscissa is rest frame wavelength, ordinate is flux normalized at 5100 Å. The dark-green line traces Fe II emission. The strongest emission features are labelled.

(Mg II absorption band was not detected), as well as Fe II templates in both the optical and UV. We use the Fe II templates obtained by Marziani et al. (2009) for the Hβ spectral region and Bruhweiler & Verner (2008) for the UV. The SPECFIT task then scales and chooses an optical broadening factor for the template that minimizes χ^2. The χ^2 minimization procedures involve all components (continuum, Fe II, emitting line components, etc.) simultaneously in order to construct a model of the spectrum. This allows us to consider the [O III] λ4959 and[O III] λ5007 lines with proper physical constraints (same shift and FWHM and a ratio 1:3; Dimitrijević et al. 2007), and to avoid any subjectivity in the placement of continuum. Spectral coverage was wide enough to ensure that a portion of continuum with no or faint emission features was available to the fitting routine. Since we are mainly interested in a detailed reproduction of line profiles, a local continuum was fitted for each spectral region considered in this study. Fig. 4 shows the continuum and Fe II placement from the SPECFIT analysis of the Hβ spectral range as an example of our approach. The fitting routine allows for the pseudo-continuum created by Fe II emission, and the fitted spectral range is wide enough to include wavelength intervals where the pseudo-continuum is low. Note that the continuum and Fe II emission were not set a priori, but computed in the same minimum χ^2 fits that allowed us to retrieve Hβ and other emission line parameters. Line fits (after continuum subtraction) are shown in Fig. 5. All fits were carried out over a wide wavelength range; however, we show four windows restricted to a lower range of the Hβ (CAHA), Mg II λ2800 (CAHA), C III] λ1909 blend(FOS) and C IV λ1549 (FOS) centroids to facilitate comparison. Residuals are shown below each fit.

We used a window from 4200 to 5500 Å to fit Hβ which include Hγ+[O III] λ4363, He II λ4686 and O[III] λλ4959,5007. Fits (see Fig. 5a) assume that [O III] λ4959 and [O III] λ5007 have the same FWHM for narrow and blueshifted semibroad components and that their flux ratio is [O III] λ4959/[O III] λ5007 = 1/3. Two components, narrow (NC) and broad (BC), were considered to model Hβ. We also fit H γ assuming the same number of components (narrow and broad) as Hβ (and same FWHM values). From the Hβ fits, we also obtain an optical Fe II flux (99×10^{-15} erg s^{-1} cm^{-2}) that together with measures of Hβ (95×10^{-15} erg s^{-1} cm^{-2}) yields an estimate of 4DE1 parameter $R_{\rm Fe\,II}$ (∼1).

Modelling of Mg II λ2800 used a 2600–3050 Å window where only this blend was detected. Each line of the Mg II λ2800 doublet was fitted by assuming broad, narrow and semibroad blueshifted components (Fig. 5b). The spectral window 1720–1960 Å includes C III] λ1909 Si II λ1814 (in yellow), Al III λ1860 (in dark green), Si III] λ1892 (in orange) and Fe III λ1914. FWHM of BCs of Si II λ1814, the doublet of Al III λ1860, and Si III] λ1892 are assumed to have the same value as C III] λ1909. We also assume an NC for C III] λ1909. For the sake of comparison, we expand the window to 2045 Å in Fig. 5(c).

The C IV λ1549 model (Fig. 5d) includes unshifted and blue components (in black and blue, respectively) and the fits to N IV] λ1486 (in cyan), Si II λ1533, He II λ1640 and O III] λ1663. We assume that He II λ1640 also shows broad and blue components (shown in brown and violet, respectively) with the same FWHMs and shifts as broad and blue C IV λ1549. All these measurements are listed in Table 3 where we include measures of equivalent width, flux, FWHM and shift (with respect to the NC). We give broad, blue and total fitting parameters for C IV λ1549. Reported uncertainties have been computed by measuring the effect, on each parameter, of the change of continuum placement. To do that we repeat the SPECFIT analysis changing the continuum by +/− 1 sigma level, that for the S/N accounted in the spectra means 2–3 per cent. We also add quadratically the formal fitting error provided by SPECFIT. The corresponding uncertainties are in agreement with those obtained for similar S/N data by Marziani et al. (2003a, b), Negrete et al. (2013, 2014) and Marziani & Sulentic (2014). For the heavily blended lines at 1900 Å, FWHM and intensity uncertainties were estimated through a χ^2 analysis of a mock spectrum with the same S/N and intensity ratio and line width (as done in Negrete et al. 2014).

3 RESULTS

3.1 3C 57: a steep spectrum RL source

3C 57 shows strong radio emission with $\log L_{1415\,\rm MHz} = 34.4$ erg s^{-1} (Griffith et al. 1994) and $R_{\rm K}$ ∼1400 (see Table 4). Both parameters indicate a classical RL quasar. 3C 57 has been a dangerous source in the past because of its compact structure leading to inclusion in samples of CD sources (Wills et al. 1992) while its steep spectrum (SS: $\alpha = -0.7$) warned that it was resolved (Morganti, Killeen & Tadhunter 1993). More recent VLA maps (Reid, Kronberg & Perley 1999) finally resolved the central core source into an elongated structure. The optical position of the quasar lies near the centre (see Fig. 6) of the elongated source suggesting that it could be an LD RL with lobe separation of ∼1.5 arcsec. If the two peaks are interpreted as lobes, then the flux ratio suggests some degree of alignment towards our line of sight. If the quasar coincides with the weaker (north) peak, then a CJ morphology would be implied putting it in the same class as PKS 1252+11. The small separation (17 kpc projected) also suggests either a preferred alignment and/or a young LD. A satellite component about 15 arcsec distant may be the relic of a past outburst. It shows no connection to the central elongated source which contains the bulk of the radio flux.

3C 57 is not included in the 470 brightest SDSS-DR quasar sample because it lies outside the SDSS fields. It is useful to compare it with the ∼46 LD RL sources in the SDSS-DR5 sample. Considering the distribution of all these sources in the plane defined by optical and radio luminosities ($\log L_{\rm bol}$ versus $\log L_{1.4\,\rm GHz}$; see fig. 6 in Z08), we find that 3C 57 is located in the upper-right corner revealing extreme radio and optical properties relative to this local RL sample. Actually, the bolometric luminosity of 3C 57 ($\log L_{\rm bol} \approx 46.98$) is higher than all 470 sources in the SDSS-DR5

Downloaded from https://academic.oup.com/mnras/article-abstract/450/2/1916/983345 by guest on 12 March 2020

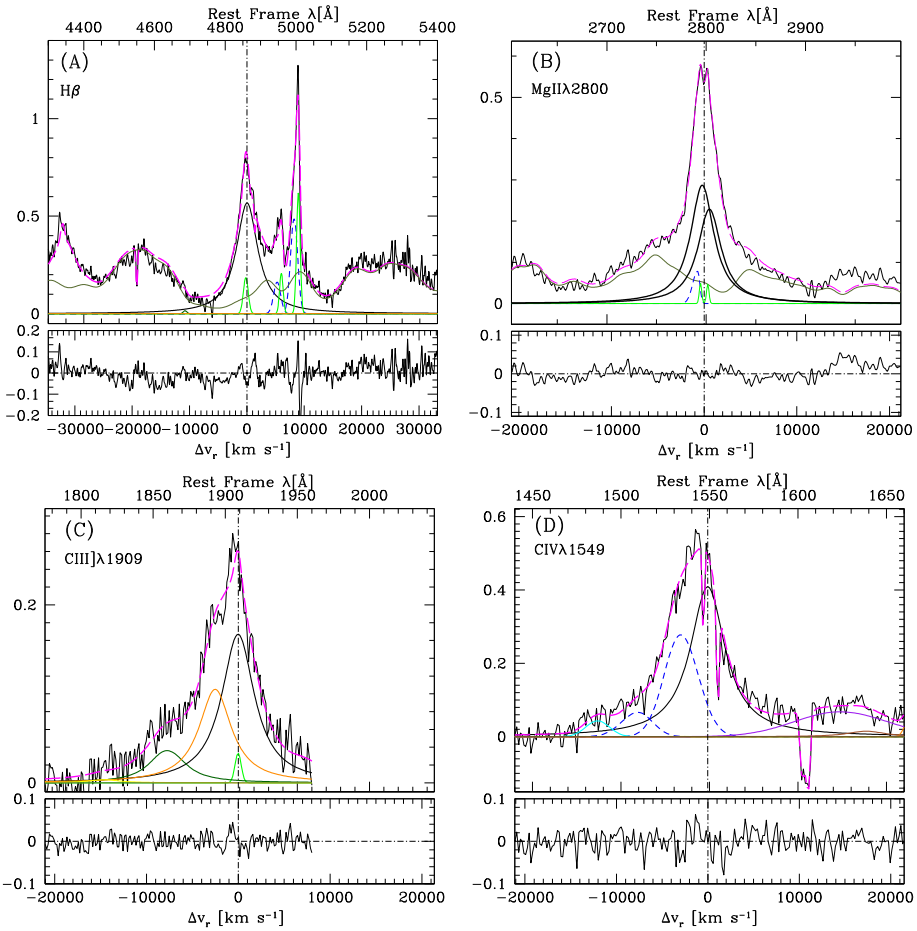


Figure 5. Multicomponent fits for 3C 57. Hβ and Mg II λ2800 from CAHA spectrum and C III] λ1909 and C IV λ1549 from *HST* spectrum. The upper abscissa is rest-frame wavelength in Å, the lower abscissa is in radial velocity units and the ordinate is specific flux per unit wavelength in arbitrary units. The vertical long dashed line indicates the adopted rest frame. The black lines show the original continuum-subtracted spectra while the dashed magenta indicates the fit to the entire spectrum. The thick black and thin green lines show the broad and narrow components, respectively. The blue-shifted component is indicated by a dashed blue line when detected. The light grey lines trace Fe II$_{UV}$ and Fe II$_{opt}$ emission which is considered in all four fittings. In some of them (as Hβ and Mg II λ2800), the contribution is very important but in others (as C III] λ1909 and C IV λ1549) it is negligible. In panel (C), apart of C III] λ1909 we show Si III] λ1892, Al III λ1860 and Si II λ1814 in orange, dark green and yellow, respectively. In panel (D), together with C IV λ1549 we plot the N IV] λ1486 component in cyan and the He II λ1640 broad and blue component in brown and violet, respectively.

Table 3. Optical and UV measurements.

Obs.	EW (Å)	Flux[a]	FWHM[b]	Shift[b]
[O III] λ5007	8	13 ± 1	725 ± 57	+187
[O III] λ5007$_{BLUE}$	12	20 ± 2	1426 ± 145	−535
Hβ_{BC}	62	95 ± 10	4500 ± 470	+223
Fe II λ4570	56	99 ± 10	–	–
Mg II λ2800$_{BC}$	25	122 ± 10	3056 ± 245[c]	+189
C III] λ1909$_{BC}$	11	177 ± 17	4318 ± 430	0[d]
Si III] λ1892$_{BC}$	7	110 ± 18	4318 ± 430	0[d]
Al III λ1860$_{BC}$	3	39 ± 12	4318 ± 430[c]	+248
C IV λ1549$_{Tot}$	26	567 ± 57	6714 ± 673	−1454
C IV λ1549$_{BC}$	17	376 ± 32	4627 ± 398	+51
C IV λ1549$_{BLUE}$	9	200 ± 26	4729 ± 602	−3034

Notes. [a]In units of 10^{-15} erg s^{-1} cm^{-2}. [b]Relative to the central wavelength of the NC in km s^{-1}. [c]FWHM of a single BC. [d]Fixed.

sample. In the upper corner of this plane, we find the most luminous CD RL quasars which are the best candidates for relativistically boosted sources while LD in this corner are the best candidates for young RL sources. Our motivation for new radio observations was to search for variability which might be expected if 3C 57 (or PKS 1252+11) were an aligned CD source. The 5 GHz specific fluxes reported in Table 2 show no evidence for changes in radio power over 30+ years. The high and stable radio power favours the idea that 3C 57 is a young LD quasar (instead of a relativistically boosted source) oriented with jet lobe axis far from our line of sight. Since the radio power did not change, we can assume that the large radio power and the unusually large C IV λ1549 blueshift coexist at the same time. Spectral index and linear size of 3C 57 meet defining criteria for CSS sources (O'Dea 1998). Absence of variability and resolved double radio morphology are consistent with 3C 57 as a young somewhat aligned LD source.

The new and older radio observations for PKS 1252+11 (Table 2) show evidence for possible changes (fading) consistent with its flat spectrum (FS) CD morphology.

3.2 Optical and UV properties

The new spectroscopic measurements confirm that 3C 57 shows mixed characteristics of a Pop A ($R_{Fe\,II} \approx 1$) and Pop B (FWHM Hβ = 4500 km s^{-1}) source. Coming back to Fig. 1 the marked

Downloaded from https://academic.oup.com/mnras/article-abstract/450/2/1916/983345 by guest on 12 March 2020

Table 4. Object from Sulentic et al. (2007) with a C IV λ1549 blueshifts ≤ -1000 km s^{-1}.

Name	4DE1 parameters					Accretion parameters				RL parameters			
	FWHM Hβ_{BC} (km s^{-1})	$R_{Fe\,II}$	Shift (km s^{-1})	$Shift_{Norm}$	Γ_{soft}	EW(C IV) (Å)	log L (erg s^{-1})	log M_{BH} ($M_\odot$)	log L/L_{Edd}	log R_K	log P (erg s^{-1}Hz^{-1})	Morph.[a]	α	Sep. (arcsec)
3C 057	4500	1.0	−1454	−0.32	2.28	18	46.83	8.98	−0.26	3.078	33.71	SS LD/CJ	−0.58	1.50
Pictor A	18400	0.01	−1110	−0.06	2.34	176	43.72	8.51	−2.90	4.217	32.60	SS LD	−1.58	480.00
PKS 1252+11	3600	0.90	−1570	−0.44	1.88	23	46.85	8.99	−0.25	2.971	33.56	FS CJ	−0.16	0.03
PKS 1355-41	8978	0.10	−1070	−0.12	1.96	74	46.13	9.17	−1.15	2.856	33.34	SS LD	−0.82	48.00
3C 390.3	12688	0.12	−1285	−0.10	1.8	132	44.83	8.78	−2.06	3.450	32.48	SS LD	−0.78	210.00
PKS 2349-01	5805	0.20	−1170	−0.20	2.44	291	45.78	8.60	−0.94	2.961	32.59	SS LD	−0.74	18.00

Note. [a]SS LD corresponds to steep spectrum lobed dominated and FS CJ corresponds to flat spectrum core jet.

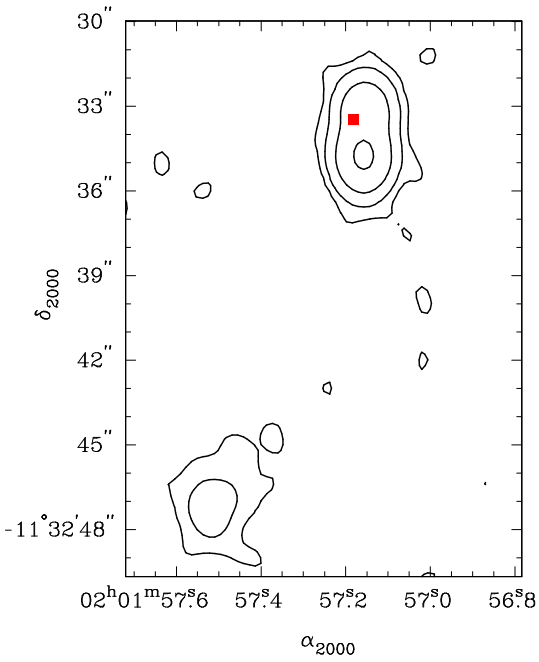


Figure 6. Contour image of the VLA maps obtained by Reid et al. (1999) at 5 GHz with a resolution of 2 arcsec. We plot levels $6 \times 10^{-4} \times$ (1, 10, 100 1000) Jy. The 3C 57 positions from the PPMXL catalogue is marked in red (Roeser, Demleitner & Schilbach 2010). The optical/NIR position is consistent with being between the two radio blobs or closer to the fainter one.

CD RL are the sources most likely connected to the LD parent population in an orientation–unification scenario. If the radio axis is oriented perpendicular to a broad line emitting accretion disc in such a scenario, the CD tend to show smaller FWHM Hβ and stronger Fe II expected if the disc is oriented closer to face-on. 3C 57 is clearly an outlier in this plot. Technically it falls in 4DE1 bin B2 (Sulentic et al. 2002), but the bin boundaries shift upwards for higher luminosity quasars (Marziani et al. 2009). The bolometric luminosity of 3C 57 is high enough to place it in bin A2 which would be more consistent with measured $R_{Fe\,II}$ and C IV λ1549 shift values. We do not detect a significant Mg II λ2800 blueshift which is also consistent with bin A2 quasars (Marziani et al. 2013a, blueshifts are most common in bin A3/A4 sources). The C IV λ1549 profile shows an outflow-dominated profile that can be fitted with: (1) a symmetric BC (assumed equal to the scaled and shifted Hβ profile) plus (2) a strong excess on the blue side – modelled here using two Gaussians.[1] Our reanalysis of the UV spectrum (more detailed than the one carried out in 2007) confirms a large shift amplitude (typical of extreme Pop A sources) with total profile shift at FWHM $c(\frac{1}{2}) = -1454$ km s^{-1}and a shift of the modelled blue component of ≈ -3000 km s^{-1}(Table 3).

Another difference between Pop A and Pop B sources involves the shape of broad Hβ. Pop A and Pop B profiles are best fitted with Lorentzian and (double) Gaussian models, respectively. Given that the optical/UV data are consistent with a Pop A source, we report in Table 3 intensity values derived from Lorentzian fits. Normalized C IV λ1549 blueshifts with amplitude greater than 1000 km s^{-1}are

[1] Note that the total excess with respect to the BC is assumed to model the radial component of the wind/outflow. Its shape offers an observational constraint for outflow models. No meaning can be ascribed to the individual Gaussian components used to model the blue excess.

Downloaded from https://academic.oup.com/mnras/article-abstract/450/2/1916/983345 by guest on 12 March 2020

relatively frequent among largely RQ Pop A sources (Fig. 2). They are rare among RL sources not only at low z but also at high z for sources of similar luminosity (Sulentic et al. 2014). Higher luminosity ($\log L_{\rm bol} \geq 47$) RL quasars no longer exist in the local Universe. Results for high-redshift quasars from an SDSS analysis suggest that C IV λ1549 blueshifts may be much more common even among RL sources (Richards et al. 2011). At lower z or L, as can be seen in Fig. 2, there is a strong concentration of mostly Pop B RL around mean values $R_{\rm Fe\,II} = 0.2$ and $c(\frac{1}{2}) = 0$ km s^{-1}. The RQ Pop A sources show a much wider parameter space dispersion towards larger $R_{\rm Fe\,II}$ and C IV λ1549 blueshifts. 3C 57 in this plot (and PKS 1252+11) is located in the Pop A domain and shows the most extreme properties for an RL quasar in the *HST* low-z sample.

3C 57 was monitored in the Catalina Real-time Transient Survey (Drake et al. 2012) for almost seven years (from JD 537 05.207 24–562 50.552 67). No large V magnitude variations were detected with an average V magnitude (computed from 269 observations) $m_V = 16.061 \pm 0.09$. The rms scatter was 0.09 which is comparable to the quoted uncertainty of individual measurements (0.08–0.1). There is evidence for small amplitude non-random variability (possibly sinusoidal, amplitude 0.1), but a more detailed study would be needed. There is no observational evidence of a significant change in the line profiles in our spectra. We verify this by scaling the NOT and CAHA spectra that cover Hβ, and the CAHA and Asiago spectra that cover Mg II λ2800. A difference between CAHA and NOT on the red side is due to the poor correction because of telluric absorption in the NOT. The Asiago spectrum is not well corrected for atmospheric extinction at its blue end. The line profiles look consistent if data quality is taken into account.

3.3 RL sources with large C IV λ1549 blueshifts

3C 57 is not unique as an RL source showing a significant C IV λ1549 profile blueshift. It is one of six RL sources in the *HST*-FOS archive with C IV λ1549 blueshift $c(\frac{1}{2}) < -1000$ km s^{-1} (Sulentic et al. 2007). Observational properties are presented for these sources in Table 4. For each object, we list the 4DE1 parameters (FWHM H$\beta_{\rm BC}$, $R_{\rm Fe\,II}$ C IV λ1549 shift, the normalized shift using FWHM H$\beta_{\rm BC}$ and $\Gamma_{\rm soft}$), EW(C IV λ1549), accretion parameters ($\log L_{\rm bol}$, $\log M_{\rm BH}$ and $\log L/L_{\rm Edd}$) and the radio properties ($\log R_{\rm K}$ $\log P_{\rm 20cm}$, morphology, spectral index (α) and lobe separation). The 4DE1 parameters and EW(C IV λ1549) were taken from Sulentic et al. (2007). In the case of 3C 57, we have recalculated FWHM H$\beta_{\rm BC}$, $R_{\rm Fe\,II}$, C IV λ1549 shift and EW(C IV λ1549) using the new data. In the accretion parameters, the bolometric luminosity ($\log L_{\rm bol}$) is estimated from the luminosity at 5100 Å assuming the standard bolometric correcting factor (10; Richards et al. 2006), the $M_{\rm BH}$ have been computed with the L-FWHM scaling from Vestergaard & Peterson (2006).

The radio parameters for 3C 57 and PKS 1252+11 have been updated to the values derived in this paper while those for the remaining objects have been calculated from the best available data in the literature (Faint Images of the Radio Sky at Twenty-cm (FIRST) data preferred).

The sources in Table 4 show a large diversity in 4DE1 optical/UV/X-ray measures as well as radio properties. Four of them fall in the Pop B optical domain of 4DE1 as expected for RL sources. The two associated with sources showing FWHM H$\beta > 10\,000$ km s^{-1}(Pictor A and 3C 390.3) cannot be usefully compared with 3C 57 since they show such broad, and occasionally double-peaked, profiles. If we normalize the C IV λ1549 shift by either FWHM H$\beta_{\rm BC}$ or FWHM C IV λ1549$_{\rm BC}$, the shift of such sources becomes much less significant compared to 3C 57. The normalized C IV λ1549 shifts of the two other Pop B sources (PKS 1355-41 and PKS 2349-01) also become less prominent after normalization. The source that remains most similar to 3C 57 is PKS 1252+11 (Fig. 2) which also shows strong Fe II placing it outside of the Pop B domain. Five of six sources in Table 4 show SS radio Spectral Energy Distributions (SEDs) and double-lobe morphology. The exception is PKS 1252+11 with a FS and CJ morphology. CD sources come in two flavours. Those with steep (CSS) and flat (FS/CS) radio SEDs. The former and latter are sometimes referred to as 'young' and 'frustrated' radio sources, respectively. The former are interpreted as birthing LD sources (e.g. van Breugel, Miley & Heckman 1984) while the latter might be failed attempts to generate LD sources, frustrated by a spiral host galaxy morphology (Fanti et al. 1995) or perhaps an unfavourable BH spin. 3C 57 appears to be a good candidate for a young LD.

Three of the sources in Table 4 can be argued to show 'young' radio morphology – two (3C 57 and PKS 2349-01) with very closely spaced LD structure and PKS 1252+11 interpreted as an LD precursor or dying frustrated source. The other three LD sources show wide enough lobe separations to preclude the assumption of a recent outburst. If we focus on 3C 57 and PKS 1252+11 as the sources with largest normalized C IV λ1549 shift, then we can argue that these sources should be considered separately from the others. The outburst age might be related with the surprisingly large C IV λ1549 outflows where the RL activity has not yet disrupted the wind. In such a scenario we assume that the scarcity of large C IV λ1549 blueshifts in RL sources, compared to RQ where they are common, involves quenching of the outflows by the onset of radio activity.

For the sake of comparison, one can also consider superluminal 3C 273 arguably the first quasar. It shows $\log(P_{\rm 20\,cm}) \backsim 34.31$ erg s^{-1} Hz^{-1} similar to 3C 57 with a CJ (or core-lobe) morphology similar to PKS 1252+11. The C IV λ1549 shift $c(\frac{1}{2}) = -552$ km s^{-1}while $R_{\rm Fe\,II} = 0.57$ and FWHM H$\beta \sim 3500$ km s^{-1} places it in bin A2 of the 4DE1 optical plane. These properties make 3C 273 a Pop A source consistent with the interpretation that is an aligned LD with undetected far-side lobe. In the optical plane of 4DE1 (Fig. 1), it lies at the transition region between LD and CD sources. One can search for additional RL sources showing large C IV λ1549 shifts in the SDSS archive. The catalogue of Shen et al. (2011) reveals (among 2347 RL quasars with $R_{\rm K} > 100$ and $z \geq 1.4$) a total of 43 sources with C IV λ1549 blueshifts $c(\frac{1}{2}) \geq 2000$ km s^{-1}. Visual examination of the spectra suggests that perhaps 10 have high enough S/N to make the blueshift credible and to tentatively assign them (using the UV criteria of Negrete et al. 2014; Marziani & Sulentic 2014) to 4DE1 bins A2/A3. 3C 57 is not unique but apparently belongs to a tiny minority of RL sources showing significant C IV λ1549 blueshifts and extreme (high $L/L_{\rm Edd}$) bin A2/A3 properties.

4 DISCUSSION

4.1 C IV λ1549 blueshifts and RL quasars

Low-redshift quasar samples (Sulentic et al. 2000a; Marziani et al. 2003a; Zamfir et al. 2010) show LD RL sources occupying a restricted zone in Eigenvector space (Fig. 1). RL sources are largely what we call Pop B quasars which are characterized by (1) broad Balmer line profiles (FWHM H$\beta > 4000$ km s^{-1}), (2) weak Fe II optical emission ($R_{\rm Fe\,II} < 0.5$), (3) absence of a C IV λ1549 blueshift and (4) absence of a soft-X-ray excess. RQ sources sharing the Pop B zone with the RL also show weak or absent C IV λ1549 blueshifts (Kuraszkiewicz et al. 2004; Sulentic et al. 2007). Perhaps

Downloaded from https://academic.oup.com/mnras/article-abstract/450/2/1916/983345 by guest on 12 March 2020

the absence of C IV λ1549 blueshifts is related to Pop B rather than to radio-loudness, or perhaps the RQ Pop B sources are pre/post-cursors of RL activity. Do they all possess the same trigger (BH spin and/or host galaxy morphology) that enables radio-loudness?

There is of course also the issue of quasar luminosity. A recent comparison between low-z sources (*HST*-FOS spectra) and 20 quasars at $z \sim 2.3 \pm 0.2$ using the GTC (in a narrow bolometric luminosity $\log L \approx 46.0 \pm 0.5$ erg s^{-1} range; Sulentic et al. 2014) shows no evidence for significant C IV λ1549 blueshifts in either sample. Apparently, C IV λ1549 blueshifts are not common in Pop B sources below $\log L < 46.5$ erg s^{-1} and are possibly even rarer in RL sources. Is C IV λ1549 blueshift correlated with source luminosity? Our main study (Sulentic et al. 2007) – that has the considerable advantage of reliable rest frame estimations based on narrow emission lines – suggests that the answer is 'no'. 4DE1 parameters do not directly correlate with source luminosity which was found to be an Eigenvector 2 parameter (Boroson & Green 1992). All of our studies involving low-z samples, and also a higher redshift VLT sample of 53 quasars (Marziani et al. 2009), point towards Eddington ratio as the principal driver of 4DE1 diversity and hence of the C IV λ1549 blueshift. The Pop A end of the 4DE1 main sequence shows systematically higher values of Eddington ratio than the Pop B end. Indeed, we find that 3C 57 shows an unusually high Eddington ratio for an RL quasar (Table 4).

Why do large SDSS samples (Richards et al. 2011) point towards a near ubiquity of C IV λ1549 blueshifts including, albeit smaller, C IV λ1549 blueshifts in the majority of RL quasars? Our mean/median C IV λ1549 blueshift (-600 ± 100 km s^{-1}) values for RQ sources is in general agreement with their SDSS results in the $\log L = 45$–47 erg s^{-1}range. The systematic discrepancy appears in RL sources. The explanation can be due two effects: (1) they do not use the improved redshift determinations from Hewett & Wild (2010) for RLs (only for RQ) and (2) they use the old definition for the RQ–RL boundary $R_K = 10$. As explained earlier, we adopt $R_K = 70$ (and/or $\log L_{1415\,\mathrm{MHz}} = 31.6$ erg s^{-1} Hz^{-1}) for this boundary. In Fig. 1, we adopt a more extreme boundary ($\log L_{1415\,\mathrm{MHz}} = 32.0$ erg s^{-1} Hz^{-1}) for RL CD sources only – under the assumption that marginally strong CD sources are unlikely to be aligned LDs. We argue that the pure CD population between $R_K = 10$ and 70 are not classical RLs. Many may be LD precursors but they are still growing. There are a lot of sources in Richards et al. (2011) with R_K between 10 and 70. If our interpretation is correct, then we expect them to show C IV λ1549 properties similar to the RQ majority. This would add a large number of C IV λ1549 blueshifts to the 'RL' population that do not belong there. A new and larger SDSS-based sample of LD sources (Kimball et al. 2011) fully confirms our adopted $\log L_{1415\,\mathrm{MHz}}$ RL limit.

4.2 The nature of 3C 57 and implications for the RQ/RL dichotomy

The outstanding property of 3C 57 involves the coexistence of a large C IV λ1549 blueshifts with a RL source showing young CJ (or aligned LD) structure. This implies that powerful relativistic ejection and a high-ionization wind, thought to be associated with the accretion disc, can coexist. It also implies that powerful radio emission can occur in a quasar radiating at a relatively high Eddington ratio. This goes against previous arguments that powerful radio emission is unsteady, or even impossible at high L/L_{Edd} (Fender & Belloni 2004; Neilsen & Lee 2009; Ponti et al. 2012). Those theoretical arguments are however based mainly on Galactic BH X-ray binaries, and it is not obvious that a close analogy with quasars can be made. It also appears to violate 4DE1 empiricism (Fig. 1) where RL sources occupy the low L/L_{Edd} end of the quasar main sequence.

The two main emission components in 3C 57 (at 5 GHz) show a projected separation of ≈17 kpc which is approximately twice the effective radius ($R_e \approx 8$ kpc; Kotilainen & Falomo 2000) inferred for the host galaxy. The projected linear size is consistent with a CSS SED source showing kpc-scale radio emission comparable to the size of the host galaxy. The development of extended (LD) radio emission requires a time $t \sim 3 \times 10^7 (v_s/0.01c)^{-1} (R/100\,\mathrm{Kpc})$ yr, where $v_s \sim 0.01c$ is the speed at the working surface of the jet (Krolik 1999, p. 298), and R is the separation between the two lobes then $t \sim 5 \times 10^6$ yr in the case of 3C 57. The central BH mass is estimated to be $\sim 10^9$ M$_\odot$ (Table 4) with an efficiency of 0.07 (Netzer 2013). The time needed for growing to this mass value is $\approx 6 \times 10^7$ yr if the source has been constantly accreting matter at a rate of ≈17 M$_\odot$ yr^{-1} – implied by the observed L/M_{BH} ratio ($\log L/L_{\mathrm{Edd}} \approx -0.26$). The accretion time-scale is an upper limit that includes the possibility of re-igniting the RL quasar activity.

Wu (2009a) found that CSS sources exhibit a rather high median value of $\log L/L_{\mathrm{Edd}}$ ($= -0.56$) that is typical of the A2 spectral region (-0.52) following Marziani et al. (2013b). Wu (2009b) suggested that a relatively short duty cycle is triggered by a radiation pressure instability within an optically thick, geometrically thin accretion disc (Czerny et al. 2009). In this interpretation, the detached radio component seen about 15 arcsec away from quasar may be a relic of past activity cycles.

The optical and UV spectra of 3C 57 are consistent with a scenario usually associated with Pop A sources of spectral types A2/A3 i.e. young or rejuvenated sources in the 4DE1 scheme. The wide majority of these sources are RQ and associated with higher accretion rates, enhanced star formation and chemical enrichment (Marziani et al. 2001; Sani et al. 2010; Marziani & Sulentic 2014). These are the sources that most frequently show a C IV λ1549 blueshift in excess of -1000 km s^{-1}. Zamanov et al. (2002) suggest that O[III] λλ4959,5007 blueshifts are also associated with the high-ionization outflow originating in these highly accreting sources. 3C 57 is not a blue outlier; however, the [O III] λ5007 profile shows a striking blueward asymmetry that can be modelled assuming a core plus semi-broad component with a relatively large blueshift. This is at variance with evolved Pop B LD Fanaroff–Riley II sources that show large EW [O III] λ5007 along with a narrow and symmetric core that appears to be consistent with dominance of the gravitational field of the host spheroid (e.g. Boroson 2003; Marziani et al. 2003b; Marziani, Dultzin-Hacyan & Sulentic 2006; Buttiglione et al. 2011). The relatively low equivalent width of [O III] λ5007 as found in 3C 57 has also been associated with a relatively young, not fully developed narrow line region (Zamanov et al. 2002; Komossa et al. 2008).

4.3 Is the wind ubiquitous and how are outflow properties affected by radio-loudness?

The jet kinetic power can be written as

$$L_j = P_j v_j \Omega_j r^2, \quad (1)$$

where $\Omega_j r^2 = A_j$ is the front end surface of the jet of solid angle Ω_j at distance r from the BH, v_j is the jet bulk expansion velocity and P_j the jet pressure within Ω_j.

$$P_j \approx 10^2 L_{j,44} \Omega_{j,-3}^{-1} r_{0.1}^{-2} v_{j,5}^{-1}\,\mathrm{dyne\,cm^{-2}}, \quad (2)$$

where $L_{j,44}$ is in units of 10^{44} erg s^{-1} (typical RL values are $\log L_j > 44$, Gu, Cao & Jiang 2009), $\Omega_{j,-3}$ is in units of 10^{-3} sterad,

Downloaded from https://academic.oup.com/mnras/article-abstract/450/2/1916/983345 by guest on 12 March 2020

$r_{0.1}$ is r at 0.1 pc ($r_{0.1\rm pc} \approx 1000\ R_{\rm g}$ for a BH mass of 10^9 $M_\odot$) and $v_{j,5}$ is the jet bulk expansion velocity in units of 10^5km s^{-1}. $P_{\rm j}$ exceeds the thermal pressure of the broad line region (BLR) gas:

$$P = \frac{\rho kT}{\mu m_{\rm p}} = nkT \approx 1.38\,10^{-3} n_9 T_4\ {\rm dyne\,cm^{-2}} \quad (3)$$

(where ρ is the mass density, T_4 the temperature in units of 10^4K and n_9 the number density in units of 10^9 cm^{-3}), as well as the hydrostatic pressure of a column of gas like the one expected to emit the blueshifted component ascribed to the accretion disc wind:

$$P_{\rm hyd} \approx \mu n m_{\rm p} h \frac{GM}{r^2} \approx \mu m_{\rm p} N_{\rm c} \frac{GM}{r^2} \approx 0.03\ N_{c,22} M_9 r_{0.1}^{-2}, \quad (4)$$

where $N_{\rm c,\,22}$ is ambient gas column density in units of 10^{22} cm^{-2}, and M_9 is the BH mass in units of 10^9 solar masses. The first implication is that there should be a zone of avoidance close to the radio axis. A second implication is that the cocoon associated with the powerful relativistic ejection is also expected to sweep the gas within the BLR. Elementary considerations based on the model of Begelman & Cioffi (1989) would suggest a cocoon pressure in directions perpendicular to that of the jet propagation:

$$P_{\rm c} \approx (P_{\rm j} \rho v_j A_j)^{1/2}/\pi r_{\rm c}^2 \approx 3\,(L_{\rm j,44} n_9 v_{\rm j,5} \Omega_{\rm j,-3})^{1/2} r_{\rm c,0.1}^{-2}\ {\rm dyne\,cm^{-2}}. \quad (5)$$

Therefore, if the cocoon side pressure is as strong as inferred from these elementary computations (that neglects general relativistic and magnetohydrodynamical effects associated with the jet tight collimation), we expect a strong, destructive effect on a high-ionization wind, especially in the innermost BLR.

Observations of powerful RL sources reported in Section 3.3 indicate that the high-ionization outflow producing C IV λ1549 and other lines is not suppressed, even if hampered or altered. There is a different dependence on luminosity of the median and average C IV λ1549 shift in the Shen et al. (2011) data for both RQ and RL: for RL, C IV λ1549 shifts are smaller amplitude and the luminosity dependence is shallower, with shifts above −1000 km s^{-1} being very rare for RL sources (cf. Richards et al. 2011).

A first inference could be that RL activity produces a wider cone of avoidance around the disc axis: i.e. suppresses emission along radial lines of flow close to the jet axis. In this case, the outflow may be more equatorially confined giving rise to more symmetric profiles and to systematically lower shifts for RL, especially for CD RLs where the flow should be viewed pole on. It is not clear whether this is the case: the sample of Sulentic et al. (2007) is small, while Richards et al. (2011) include many core sources that may not be RL ($R_{\rm K}$ = 10–70). In this interpretation, the radio morphology of 3C 57 may hint at a favourable orientation, coupled with a significant outflow due to the high $L/L_{\rm Edd}$. Another possibility (not conflicting with the previous one) is that the wind is forced to start at larger distances from the central BH (the cocoon pressure decreases with r^{-2}) reaching a lower terminal velocity (still significantly above the escape velocity from the system). Larger emitting distances may also be consistent with the models of Zamanov et al. (2002) and Komossa et al. (2008).

Large (above 1000 km s^{-1}) C IV λ1549 blueshifts appear to be rare: the tentative estimates of Section 3.3 yield a prevalence 0.5–2 per cent. The rarity of these sources suggests another possible explanation for the 3C 57 (and PKS 1252+11) blueshift: the radio activity ignited too recently to have yet disrupted the wind. For 3C 57 ($\log M_{\rm BH} \approx 9$), the dynamical time-scale of the BLR is ∼100 yr. The derived $M_{\rm BH}$ is large; this indicates that 3C 57 is a rejuvenated quasar. If the duty cycle of rejuvenated quasars is $\lesssim 10^4$ yr (Czerny et al. 2009), then one may expect ∼1 per cent of sources whose BLR has not been yet fully affected by the onset of radio activity.

5 CONCLUSIONS

The 4D Eigenvector formalism reveals that the majority of RL quasars show a restricted zone of parameter space occupation compared to the RQ majority. This restriction is clearest when we focus on the unambiguously RL LD sources. They show restricted ranges of radio power ($\log L_{1415\,\rm MHz} > 31.6$ erg s^{-1} Hz^{-1}), bolometric luminosity ($\log L_{\rm bol} > 44.0$ erg s^{-1}), FWHM Hβ (> 4000 km s^{-1}), $R_{\rm Fe\,II}$ (<0.5), $\Gamma_{\rm soft}$(<2.5) and modest C IV λ1549 blueshifts. Since the defining 4DE1 parameters are assumed to measure aspects of BLR physics and source geometry/kinematics, this implies either (1) if all quasars are capable of radio-loudness, then important physical and/or kinematic properties of the BLR must change before the onset of a RL event or (2) as an alternative reflected in the Pop A–Pop B distinction, RL represent a distinct class of quasars driven perhaps by different BH spin and/or host galaxy morphology. The RQ sources sharing the same 4DE1 parameter domain with the RL might represent currently radio inactive Pop B quasars. We see an RQ–RL dichotomy if we consider only LD sources (as the RL parent population). CD sources are likely a mix of (rare) aligned LD sources, LD precursors and frustrated cores incapable of producing classical LD structure. CD sources above $\log L_{1415\,\rm MHz} < 32-32.5$ erg s^{-1} Hz^{-1} distribute in 4DE1 as expected if they are aligned LD (e.g. FWHM Hβ near lower limit of LD) in an orientation–unification scenario while CD with $\log L_{1415\,\rm MHz} < 32-32.5$ do not. The weaker CD sources also distribute in 4DE1 space the same as the RQ majority.

There are always exceptions to the rule. The cases of 3C 57 and PKS 1211+11 show that a prominent high-ionization outflow probably driven by radiation pressure can coexist with powerful radio emission, although the simultaneous detection of both phenomena appears to be rare. This result suggests that high accretion and relativistic radio ejection may not be mutually exclusive for supermassive BHs, as found in the case of stellar mass BHs, and, at the same time, that radio emission has a quantitative effect on the high-ionization outflows.

3C 57 shows extreme optical and radio properties compared to the local RL population and is therefore unambiguously RL ($\log L_{1415\,\rm MHz} \approx 34.4$ erg s^{-1} Hz^{-1} and $\log R_{\rm K} \sim 3$). However, it shows two 4DE1 parameters that are highly discordant with the RL majority: unusually strong optical Fe II emission ($R_{\rm Fe\,II} \sim 1$) and a large C IV λ1549 blueshift ∼ −1500 km s^{-1}. It also shows an estimated Eddington ratio ($\log L/L_{\rm Edd} \approx -0.26$) much higher than the majority of RL quasars and typical of a Population A2 source. VLA maps resolve it leading to an interpretation of 3C 57, which shows a CSS radio SED, as a CJ or aligned LD source. The radio flux stability favours a young LD quasar. The C IV λ1549 profile blueshift implies that there is a wind or outflow from a highly accreting disc. The general absence of C IV λ1549 blueshifts in RL sources suggested the onset of radio activity somehow disrupts or confines the wind. A search of the SDSS quasar catalogue suggests that 3C 57 belongs to a tiny minority of RL sources with significant C IV λ1549 blueshifts and high Eddington ratio.

It is clear that whatever the physical properties of the BLR in normal quasars, the RL show a restricted range in those properties presumably connected to their large $M_{\rm BH}$ and low $L/L_{\rm Edd}$. 3C 57 is then likely hosted by an early-type galaxy if the large BH mass implies a large bulge mass via the BH mass–bulge mass

Downloaded from https://academic.oup.com/mnras/article-abstract/450/2/1916/983345 by guest on 12 March 2020

correlation. The unusual properties are most easily understood if 3C 57 is undergoing an apparently rare major accretion event. This assumes that the rare unusually strong Fe^{II} emission in an RL is a signature of such events. This causes 3C 57 to show properties typical of the opposite end of the 4DE1 main sequence (higher BLR density, metallicity and accretion disc wind). The C IV wind is either too strong to be disrupted or the event is so recent that this disruption has not yet occurred.

ACKNOWLEDGEMENTS

We acknowledge Dra Simona Righini for observations in INAF–IRA radiotelescope station in Medicina (Italy). We would like to thank Drs Jaime Perea and Isabel Márquez for all the fruitful discussions on the subject and their help with the observations. We also thank the anonymous referee for many useful comments which helped to significantly improve the presentation of our analysis. Part of this work was supported by Junta de Andalucía through grant TIC-114 and by the Spanish Ministry for Science and Innovation through grants AYA2010-15169, AYA2011-1544-E and AYA2013-42227-P. This research is based in part on data obtained with the 1.82-m Copernico Telescope at the Asiago Observatory. Based partially on observations made with the 3.5-m telescope at the Spanish-German Observatory in Calar Alto (CAHA, Almería Spain) jointly operated by the Max-Planck-Institut für Astronomie Heidelberg and the Instituto de Astrofísica de Andalucía (CSIC). We thank all the CAHA staff for their high professionalism and support with the observations. Some data presented here were obtained with ALFOSC, which is provided by the Instituto de Astrofísica de Andalucía (IAA) under a joint agreement with the University of Copenhagen and NOTSA.

REFERENCES

Begelman M. C., Cioffi D. F., 1989, ApJ, 345, L21
Boroson T. A., 2003, ApJ, 585, 647
Boroson T. A., Green R. F., 1992, ApJS, 80, 109
Bruhweiler F., Verner E., 2008, ApJ, 675, 83
Buttiglione S., Capetti A., Celotti A., Axon D. J., Chiaberge M., Macchetto F. D., Sparks W. B., 2011, A&A, 525, A28
Corbin M. R., Smith P. S., 2000, ApJ, 532, 136
Czerny B., Siemiginowska A., Janiuk A., Nikiel-Wroczyński B., Stawarz Ł., 2009, ApJ, 698, 840
de Vries W. H., Becker R. H., White R. L., 2006, AJ, 131, 666
Dimitrijević M. S., Popović L. Č., Kovačević J., Dačić M., Ilić D., 2007, MNRAS, 374, 1181
Drake A. J. et al., 2012, Proc. IAU Symp. 285, New Horizons in Time-Domain Astronomy. Cambridge Univ. Press, Cambridge, p. 306
Fanti C., Fanti R., Dallacasa D., Schilizzi R. T., Spencer R. E., Stanghellini C., 1995, A&A, 302, 317
Fender R., Belloni T., 2004, ARA&A, 42, 317
Griffith M. R., Wright A. E., Burke B. F., Ekers R. D., 1994, ApJS, 90, 179
Gu M., Cao X., Jiang D. R., 2009, MNRAS, 396, 984
Hewett P. C., Wild V., 2010, MNRAS, 405, 2302
Kellermann K. I., Sramek R., Schmidt M., Shaffer D. B., Green R., 1989, AJ, 98, 1195
Kimball A. E., Ivezić Ž., Wiita P. J., Schneider D. P., 2011, AJ, 141, 182
Komossa S., Xu D., Zhou H., Storchi-Bergmann T., Binette L., 2008, ApJ, 680, 926
Kotilainen J. K., Falomo R., 2000, A&A, 364, 70
Kriss G., 1994, in Crabtree D. R., Hanisch R. J., Barnes J., eds, ASP Conf. Ser. Vol. 61, Astronomical Data Analysis Software and Systems III. Astron. Soc. Pac., San Francisco, p. 437
Krolik J. H., 1999, Active Galactic Nuclei : From the Central Black Hole to the Galactic Environment. Princeton Univ. Press, Princeton
Kuehr H., Witzel A., Pauliny-Toth I. I. K., Nauber U., 1981, A&AS, 45, 367
Kuraszkiewicz J. K., Green P. J., Crenshaw D. M., Dunn J., Forster K., Vestergaard M., Aldcroft T. L., 2004, ApJS, 150, 165
Laurent-Muehleisen S. A., Kollgaard R. I., Ryan P. J., Feigelson E. D., Brinkmann W., Siebert J., 1997, A&AS, 122, 235
Marziani P., Sulentic J. W., 2014, MNRAS, 442, 1211
Marziani P., Sulentic J. W., Dultzin-Hacyan D., Calvani M., Moles M., 1996, ApJS, 104, 37
Marziani P., Sulentic J. W., Zwitter T., Dultzin-Hacyan D., Calvani M., 2001, ApJ, 558, 553
Marziani P., Sulentic J. W., Zamanov R., Calvani M., Dultzin-Hacyan D., Bachev R., Zwitter T., 2003a, ApJS, 145, 199
Marziani P., Zamanov R. K., Sulentic J. W., Calvani M., 2003b, MNRAS, 345, 1133
Marziani P., Dultzin-Hacyan D., Sulentic J. W., 2006, New Developments in Black Hole Research. Nova Science Publishers, New York, p. 123
Marziani P., Sulentic J. W., Stirpe G. M., Zamfir S., Calvani M., 2009, A&Ap, 495, 83
Marziani P., Sulentic J. W., Plauchu-Frayn I., del Olmo A., 2013a, A&A, 555, A89
Marziani P., Sulentic J. W., Plauchu-Frayn I., del Olmo A., 2013b, ApJ, 764, 150
Morganti R., Killeen N. E. B., Tadhunter C. N., 1993, MNRAS, 263, 1023
Negrete C. A., Dultzin D., Marziani P., Sulentic J. W., 2013, ApJ, 771, 31
Negrete C. A., Dultzin D., Marziani P., Sulentic J. W., 2014, ApJ, 794, 95
Neilsen J., Lee J. C., 2009, Nature, 458, 481
Netzer H., 2013, The Physics and Evolution of Active Galactic Nuclei. Cambridge Univ. Press, Cambridge
O'Dea C. P., 1998, PASP, 110, 493
Oke J. B., 1990, AJ, 99, 1621
Ott M., Witzel A., Quirrenbach A., Krichbaum T. P., Standke K. J., Schalinski C. J., Hummel C. A., 1994, A&A, 284, 331
Ponti G., Fender R. P., Begelman M. C., Dunn R. J. H., Neilsen J., Coriat M., 2012, MNRAS, 422, L11
Reid R. I., Kronberg P. P., Perley R. A., 1999, ApJS, 124, 285
Richards G. T. et al., 2006, ApJS, 166, 470
Richards G. T. et al., 2011, AJ, 141, 167
Roeser S., Demleitner M., Schilbach E., 2010, AJ, 139, 2440
Sani E., Lutz D., Risaliti G., Netzer H., Gallo L. C., Trakhtenbrot B., Sturm E., Boller T., 2010, MNRAS, 403, 1246
Shen Y. et al., 2011, ApJS, 194, 45
Sulentic J. W., Marziani P., Dultzin-Hacyan D., 2000a, ARA&A, 38, 521
Sulentic J. W., Marziani P., Zwitter T., Dultzin-Hacyan D., Calvani M., 2000b, ApJ, 545, L15
Sulentic J. W., Marziani P., Zamanov R., Bachev R., Calvani M., Dultzin-Hacyan D., 2002, ApJ, 566, L71
Sulentic J. W., Zamfir S., Marziani P., Bachev R., Calvani M., Dultzin-Hacyan D., 2003, ApJ, 597, L17
Sulentic J. W., Bachev R., Marziani P., Negrete C. A., Dultzin D., 2007, ApJ, 666, 757
Sulentic J. W., Marziani P., del Olmo A., Dultzin D., Perea J., Negrete C. A., 2014, A&A, 570, A96
van Breugel W., Miley G., Heckman T., 1984, AJ, 89, 5
Vestergaard M., Peterson B. M., 2006, ApJ, 641, 689
Wills B. J., Wills D., Breger M., Antonucci R. R. J., Barvainis R., 1992, ApJ, 398, 454
Wright A. E., Wark R. M., Troup E., Otrupcek R., Hunt A., Cooke D. J., 1990, PASA, 8, 261
Wu Q., 2009a, MNRAS, 398, 1905
Wu Q., 2009b, ApJ, 701, L95
Zamanov R., Marziani P., Sulentic J. W., Calvani M., Dultzin-Hacyan D., Bachev R., 2002, ApJ, 576, L9
Zamfir S., Sulentic J. W., Marziani P., 2008, MNRAS, 387, 856 (Z08)
Zamfir S., Sulentic J. W., Marziani P., Dultzin D., 2010, MNRAS, 403, 1759
Zensus J. A., Ros E., Kellermann K. I., Cohen M. H., Vermeulen R. C., Kadler M., 2002, AJ, 124, 662

This paper has been typeset from a TEX/LATEX file prepared by the author.

Downloaded from https://academic.oup.com/mnras/article-abstract/450/2/1916/983345 by guest on 12 March 2020